Eng. Sci., 2022, **20**, 330–340

Engineered Science

DOI: https://dx.doi.org/10.30919/es8d734

Investigating the Effect of a Single Peristalsis Wave on Unobstructed Ureter Using a Computational Technique

Laxmikant G Keni,[1,#] Satish Shenoy B,[1,#] Padmaraj Hegde,[2,#] Prakashini K,[3,#] Masaaki Tamagawa,[4,#] Shah Mohammad Abdul Khader,[5,#] BM Zeeshan Hameed[6,#] and Mohammad Zuber[1,*]

Abstract

The ureter transports urine from the kidney to the bladder. During the peristalsis, the contraction of the ureter helps to move the urine in bolus form. In the current work, the ureter is modeled and a single peristalsis wave is used to know the effect of pressure and velocity at a different location in the ureter at different intervals of time for four inlet boundary conditions. A three-dimensional ureter model with 275 mm length is used in the current work. The analysis is carried out using a commercially available computational dynamic package ANSYS-CFX. A single sinusoidal peristaltic wave with a change in pressure is used for the analysis. The inlet pressure is varied as 0.1 Pa, 0.3 Pa, 0.5 Pa, and 0.7 Pa. The maximum pressure was found to be 1.28 Pa at an input pressure of 0.7Pa. In the neck region, a negative pressure of -1.03 Pa is observed at 0.1 Pa. At time T/4, it is observed that the maximum velocity of 0.0406 m/s at N1. In all the other time steps and locations, the minimum velocity of 0.017 m/s is observed. The reverse flow due to negative pressure will develop the urinary tract infection in the ureter and result in the bacteria and toxins from the ureter into the renal pelvis and kidneys.

Keywords: Peristalsis; Computational fluid dynamics; Urine reflux; Velocity; Pressure.
Received: 19 April 2022; Revised: 25 May 2022; Accepted: 27 May 2022.
Article type: Research article

1. Introduction

The transport of urine from the kidney to the bladder is a complex biological phenomenon known as peristalsis. The ureter is the muscular structure that transports urine from the kidney to the bladder. The renal pelvis collects the urine from the kidney and by the peristaltic wave motion on the ureter wall, urine is propelled to the bladder. Obstructions in the ureter constriction and vesicoureteral reflux are the two major problems that occur in the ureter, which may cause an increase in bladder pressure.[1,2] During the peristalsis, the contraction of the ureter helps to move the urine in bolus form. The increase in the urine flow rate may increase the contraction frequency and decrease the amplitude of the peristalsis.[3] Thus the ureter contracting rate and load required for contracting to define the bolus formation or the urine movement in the ureter.[4,5]

Kill[6] described that the ureteral peristaltic rate rises in most instances but may remain unaltered altogether or may fall, and concluded that there is no regularity in the ureteral response pattern to increased urine flow. Many researchers studied theoretical and experimental modeling to understand the biomechanics of peristalsis and urine propelled from the kidney to the bladder.[7–9] Burns and Parkes[10] compared the peristaltic motion for the symmetric pipe without any pressure gradient and pressure gradient represented using the sinusoidal wave to generate the peristalsis.[11,12] Bruijnes[13] investigated the functional pressure profile properties of the ureter and carried out the pressure profile study on the dogs' ureter with the polyethylene catheter. They showed constant pressure in the ureter pelvis junction (UPJ) but significant variation in pressure in the mid ureter and biphasic pressure profile in the ureterovesical junction (UVJ). Kundo *et al.*[3] documented the amplitude, frequency, and pressure of contraction during peristaltic movement and the dynamics of peristalsis of human

[1] *Department of Aeronautical and Automobile Engineering, Manipal Institute of Technology, Manipal Academy of Higher Education, Manipal, Karnataka, India.*
[2] *Department of Urology, Kasturba Medical College, Manipal Academy of Higher Education, Manipal, Karnataka, India.*
[3] *Department of Radio Diagnosis, Kasturba Medical College, Manipal Academy of Higher Education, Manipal, Karnataka, India.*
[4] *Department of Biological Functions and Engineering, Kyushu Institute of Technology, Japan.*

and dog ureter. They showed that the reverse pressure forms instantly after the progressive systolic contraction. Shafik *et al.*[14] developed the report on a measurement of ureteric pressure profiles in the normal and pathologic ureter to provide a better understanding of the urine transport mechanism from the kidney to the bladder. Their result shows that ureteric pressure fluctuated from the basal pressure to a high-pressure value during peristalsis. The numerical simulation of the ureter lumen flow is limited to simple 2D modeling and boundary conditions because of the complexity of urine transportation.[15] The mechanical properties of the ureter are one of the key factors for the fluid-structure interaction analysis.[16–19] Rassoli *et al.*[20] conducted a biaxial study of a human ureter to predict the mechanical response of the ureter tissue under complex mechanical loading conditions. They found the ureter wall behaves as anisotropic, modeled as hyperplastic material. They used modified Mooney- Rivlin elastic to formulate the constitutive ureter model. Vahidi *et al.*[21] presented the basic 2D urinary system model with FSI using real ureteral data to understand the flow behavior. In another research Nasser *et al.*[22] considered a simple axisymmetric ureter model to investigate the ureter reflux phenomenon and wall shear during the peristalsis. They showed that reflux occurs at the beginning of the peristalsis and peristalsis effectiveness is highly dependent on the ureter wall properties. Najafi *et al.*[19,23] presented and analyzed 2D and 3D models for ureter flow with and without obstruction. The velocity, pressure, and wall shear are compared for the obstruction of different-sized stones placed in the ureter to understand the effect of obstruction on the flow dynamics and ureter wall.

However, all these studies focused on the flow behavior in the ureter. This could help health providers to understand the effects of fluid dynamics on the ureter wall. In this current research, a three-dimensional model is numerically simulated to understand the pressure and velocity effect in the bolus and neck of the ureter during the peristalsis. Finite element studies have significantly influenced medical applications.[24–28] Using computational fluid, in vitro studies can be performed to analyze the functioning of human organs. This saves lots of time and can predict the actual scenario without any intervention. Nowadays Finite element method (FEM) and computational fluid dynamics are used in analyzing medical implants.[26,29,30] In the current work, the effect of peristalsis at a different location with a change in pressure and velocity is studied.

2. Material and methods

2.1 Modelling and meshing

Usually, the male ureter length will be between 150 mm to 290 mm.[31] In the present work ureter with a length of 275 mm is considered.[32] The outer diameter of 3mm and wall thickness of 1mm are considered for the ureter model and the ureter is elastic.[23] Ansys 2019-R2 is used for modeling the ureter. Fig. 1 shows the ureter modeled as the three-dimensional pipe. Ansys-CFX, a commercially available computational dynamics package is used for the analysis.

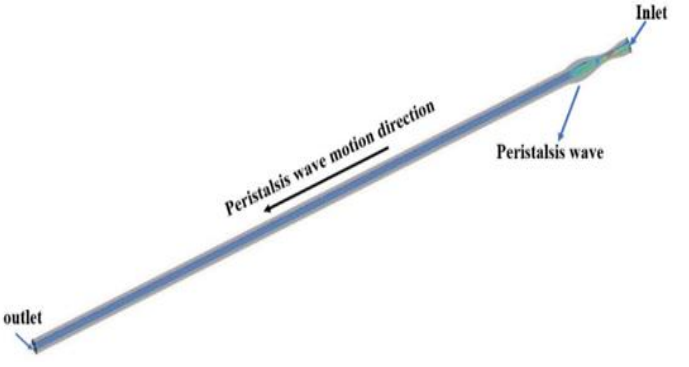

Fig. 1 Ureter geometry and direction of bolus motion.

Using the second-order upwind scheme the standard scheme, momentum and pressure, respectively are calculated.[33] Diffusion-based smoothing was adopted for mesh movement. Fig. 2 shows the meshed structure of the ureter. Ten layers of inflation are added at a 1.2 growth rate. The simulation is set for 0.01s and a total flow time of 18s is considered for the ureter flow. The final meshed model consists of a total number of elements and nodes of 2,790,000 and 2,823,381, respectively. The grid dependency study is carried out for an inlet pressure of 0.3Pa at 0.01 mesh size, and no variation in pressure values was observed.[32]

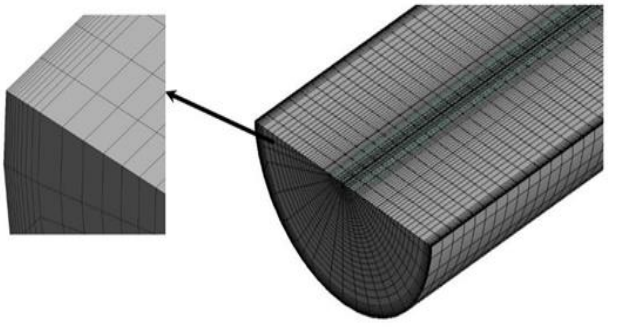

Fig. 2 Cross-section of the meshed structure of ureter.

[5] *Department of Mechanical and Manufacturing Engineering, Manipal Institute of Technology, Manipal Academy of Higher Education, Manipal, Karnataka, India.*

[6] *Department of Urology, Father Muller Medical College, Mangalore, Karnataka, India.*

[#]*These authors contributed equally to this work.*

**Email:* mohammad.zuber@manipal.edu (M. Zuber)

2.2 Boundary condition

During analysis, an inlet pressure of 0.1 Pa, 0.3 Pa, 0.5 Pa, and 0.7 Pa, and the outlet pressure of 0 Pa is applied for the ureter. No slippage and no penetration between fluid and ureteral wall are considered.[34,35] The moving ureteral wall is adopted by the wave generated according to equation 3.

2.2.1 Governing equation

Urine is considered to be a homogenous, viscous, and incompressible Newtonian fluid. The principal fluid equations are incompressible Navier- Stokes equation with a constant urine density, $\rho = 1050$ kg/m3, and viscosity, $\mu = 1.3$cP.[36]
The continuity equation is given as,

$$\nabla . u_f = 0 \quad (1)$$

The momentum equation is,

$$\frac{\partial u_f}{\partial t} + (u_f . \nabla) u_f = -\nabla p + \frac{\mu}{\rho}(\nabla^2 u_f) \quad (2)$$

Where u_f is velocity vector, p is the pressure, ρ is density and μ is fluid dynamic viscosity. The SIMPLE algorithm handles the pressure components in momentum equations and employs an iterative technique to acquire the solution to the discretized equations.[37]

2.2.2 Peristaltic motion

Sinusoidal peristaltic wave motion is applied on the ureteral wall with a physiological velocity of 20mm/sec. This velocity magnitude is used in our study because the range of peristaltic physiological velocity is varying from 20 to 60 mm/s.[38]
The ureter wall displacement is considered as per equation 3,

$$d\,(z,t) = \pm a \sin(kz) \sin(\omega t) \quad (3)$$

Where a= 1 mm, the amplitude of displacement, k= wave number (considered as 2 for a single wave), and $\omega =$ frequency (1 Hz).

3. Result and discussion

A three-dimensional ureter model was modeled and analyzed for the flow dynamics. A total wave cycle for 18s times with a wave velocity of 20 mm/s is used. Eighteen seconds is segregated with a time interval of 4.5 s. Table 1 shows the time in which pressure and velocity profiles are analyzed. The pressure and velocity profile at the center of the bolus and neck is analyzed at a time step of 0.01s.

3.1 The pressure at the center of urine bolus and bolus neck

Figure 3 shows the bolus and neck center for the four steps of T/4, T/2, 3T/4, and T s, where B1, B2, B3, and B4 are bolus center locations. similarly, N1, N2, N3, and N4 are bolus neck centers.

Under normal circumstances, the peristaltic waves ensure the propulsion of the urinary bolus toward the bladder. As the urine is collected in the renal pelvis, the pelvic pressure increases and initiates a peristaltic contraction that is propagated along the ureter to the bladder. The inlet pressure was analyzed at 0.1 Pa, 0.3 Pa, 0.5 Pa, and 0.7 Pa. Wienberg *et al.*[39] observed that the maximum pressure is generated behind the propagating urine bolus. Similar pressure was observed in the model used for the analysis.

Initially, at T/4 s, the peristalsis wave reaches locations B1 and N1, due to contraction in the neck due to peristalsis motion, maximum pressure is developed in the bolus and a negative pressure develops in the neck as shown in Fig. 4. The maximum pressure was found to be 1.28 Pa at an input pressure of 0.7 Pa (Fig. 4(a)). In the neck region, a negative pressure of -1.03 Pa is observed at 0.1 Pa. In the remaining regions, the pressure becomes almost equal to the resting pressure when the lumen has reached its minimum diameter (Fig. 4(b)). The negative pressure at location N1 indicates the reverse flow at the inlet. Lykoudis *et al.*[40] reported the rise in the pressure due to contraction in the ureter, and as the wave propagates the pressure reached normal.

Table 1. Different time intervals at which pressure and velocity profiles are analyzed.

Sl No	Time interval	Time (in seconds)
1.	T/4	0 to 4.5
2.	T/2	4.5 to 9
3.	3T/4	9 to 13.5
4.	T	13.5 to 18

As the wave propagates further with the volume of urine at time T/2s, the peristalsis wave reaches locations B2 and N2 as shown in Figs. 5(a & b). It is observed that at B2, the maximum pressure of 0.931 Pa for the input pressure of 0.7 Pa, and at N2, the negative pressure of -1.145 Pa for the input pressure of 0.1 Pa. High-pressure regions are formed downstream of the contractions as shown in Fig. 5(a). Similarly, at the 3T/4 s, the peristalsis wave reaches locations B3 and N3. The pressure recorded here is 0.622 Pa for 0.7 Pa input pressure at location B3 (Fig. 5(c)) and negative pressure of -1.327 Pa for input pressure at N3 as shown in Fig. 5(d).

Similar to previous time steps, as shown in Fig. 6(a), maximum pressure of 0.34 Pa for 0.7 Pa input pressure at B4 and the input pressure of 0.1 Pa with a negative pressure of -

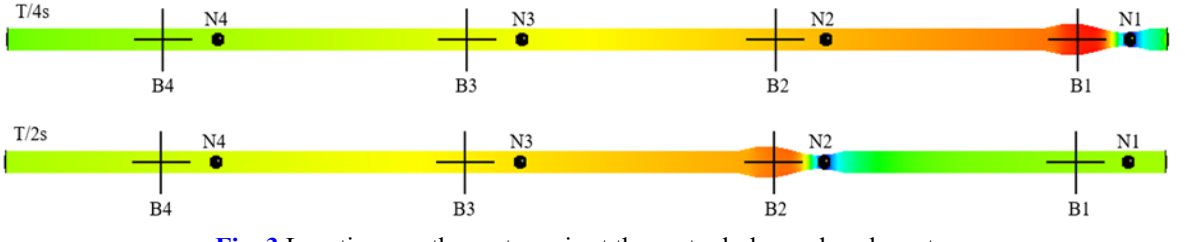

Fig. 3 Locations on the ureter axis at the ureter bolus and neck center.

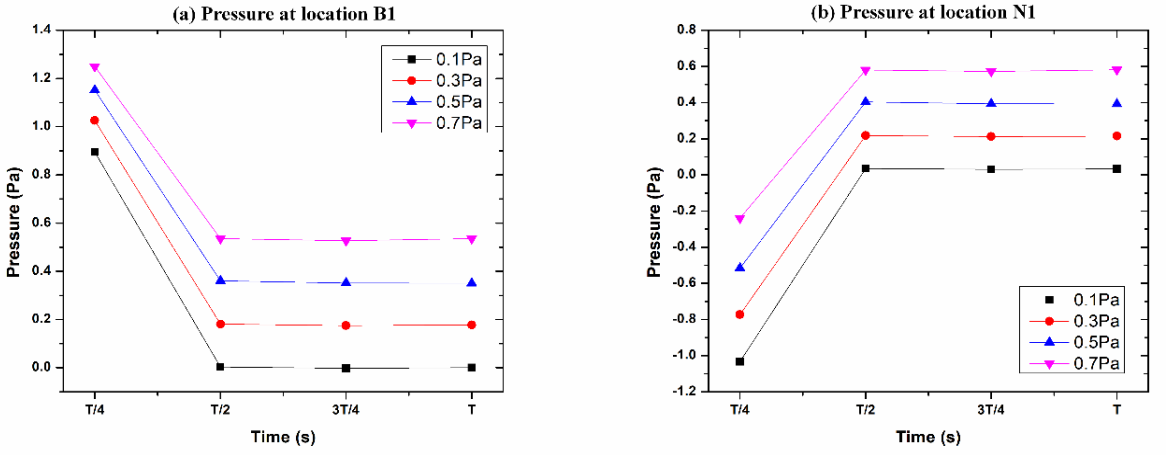

Fig. 4 (a) Pressure at bolus center B1 at time T/4 s; (b) Pressure at neck center N1 at time T/4 s.

1.512 Pa at N4 are recorded (Fig. 6(b)). This reverse flow due to negative pressure will develop the urinary tract infection in the ureter and results in the bacteria and toxins from the ureter into the renal pelvis and kidneys.[41,42] This may further lead to serious kidney problems over a period of time. The final stage of propagation is T s, as shown in Fig. 6.

It has been observed for the 0.1 Pa, 0.3 Pa, 0.5 Pa, and 0.7 Pa input pressure the maximum pressure magnitude is found at the input pressure of 0.7 Pa, and the bolus region and the minimum pressure magnitude obtained in the neck region at 0.1 Pa. To analyze, the percentage increase or decrease in the flow, input pressure of 0.1 Pa and 0.7 Pa is considered as shown in Table 2. As the wave propagates from T/4 s to T s, pressure drop of 73% is observed for the inlet pressure of 0.7Pa in the bolus. On the other hand, in the neck region, a drastic increase in the negative pressure of 43% was found for the lower inlet pressure of 0.1Pa. This indicates that there is a more tendency for reverse flow during the peristalsis motion. The pressure due to peristalsis in the neck will affect the flow in the form of reverse flow.

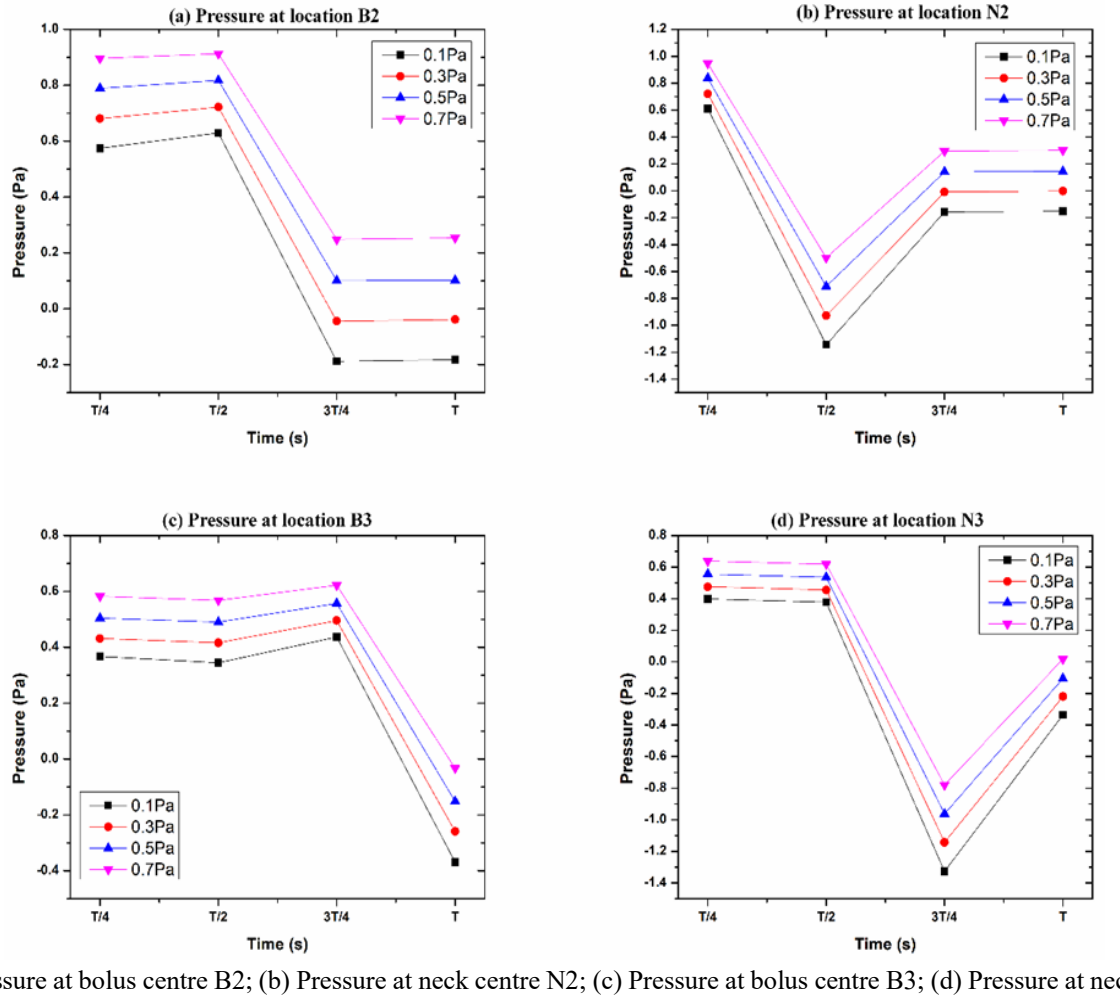

Fig. 5 (a) Pressure at bolus centre B2; (b) Pressure at neck centre N2; (c) Pressure at bolus centre B3; (d) Pressure at neck centre N3.

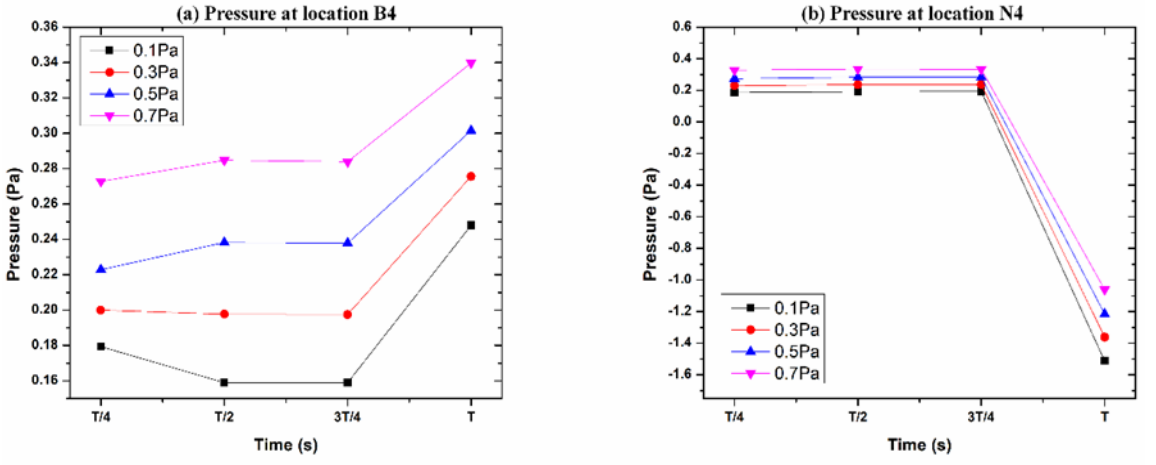

Fig. 6 (a) Pressure at bolus center B4; (b) Pressure at neck center N4.

3.2 Peristalsis wave velocity profile

The velocity profile is given a clear idea of when urine reflux takes place at the inlet. If the rate of reflux is high, then it causes serious damage to the kidneys over some time. Fig. 7 shows the flow vector streamlines for the moving bolus. As the peristalsis wave begins to move from inlet to outlet exactly at 1.4 sec (Fig. 7(a)), a high magnitude velocity and backward flow are generated at the inlet exactly at 2.9 s (Fig. 7(b)). As the peristalsis wave propagates, a large number of the backward flow is generated at the UPJ at a time of 3.5 s as shown in Fig. 7(c). Hosseini *et al.*[43] showed that the maximum shear stress on the wall depends on the velocity of the contraction in the ureter and also reported that due to fluid inertia the maximum flow occurs at the contracted region.

During the peristalsis wave motion, the inlet backward flow section was restricted to the area near the ureter axis but in a bolus of the ureter backward flow regions were prolonged to the contracted portion of the ureter. When the wave propagates to a distance of 24 mm that is at 4 s, the retrograde flow at the inlet will disappear and the reflux regions are formed as the bolus moves towards the bladder as shown in Fig. 7(d).[34]

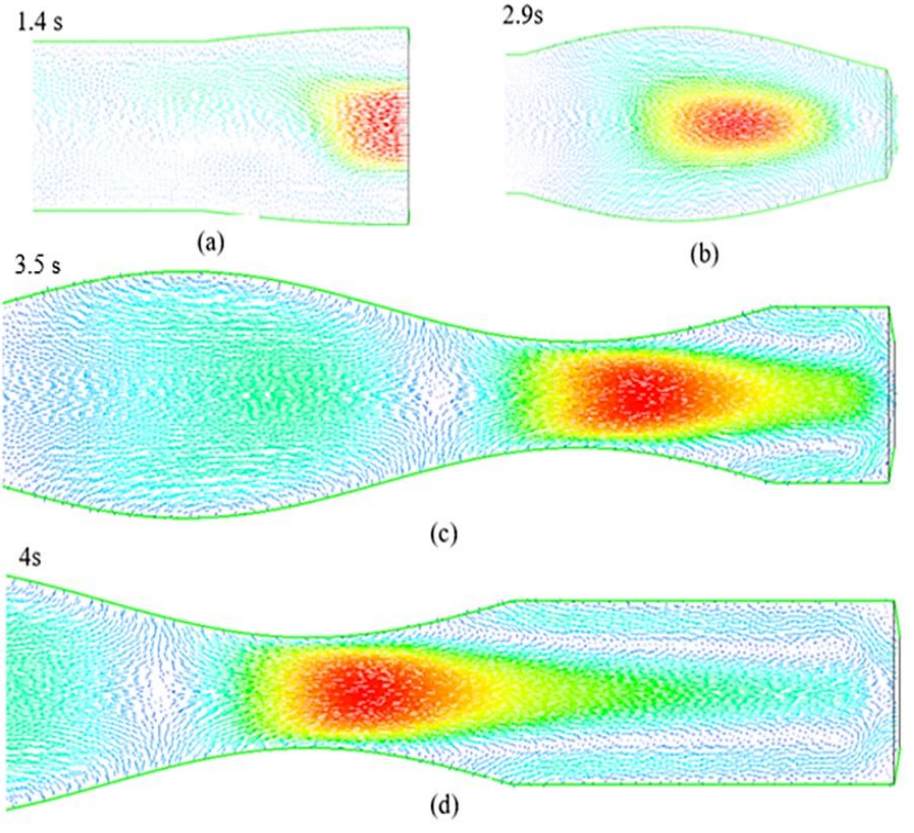

Fig. 7 Urine velocity streamlines for moving bolus. a) Peristalsis wave begins at the inlet at 1.4 s; b) At the time 2.9 s ureteral backward flow generates as peristalsis wave propagation towards the outlet; (c) The generation of the backward flow at 3.5 s; and (d) At 4 s the reverse flow will disappear at the inlet.

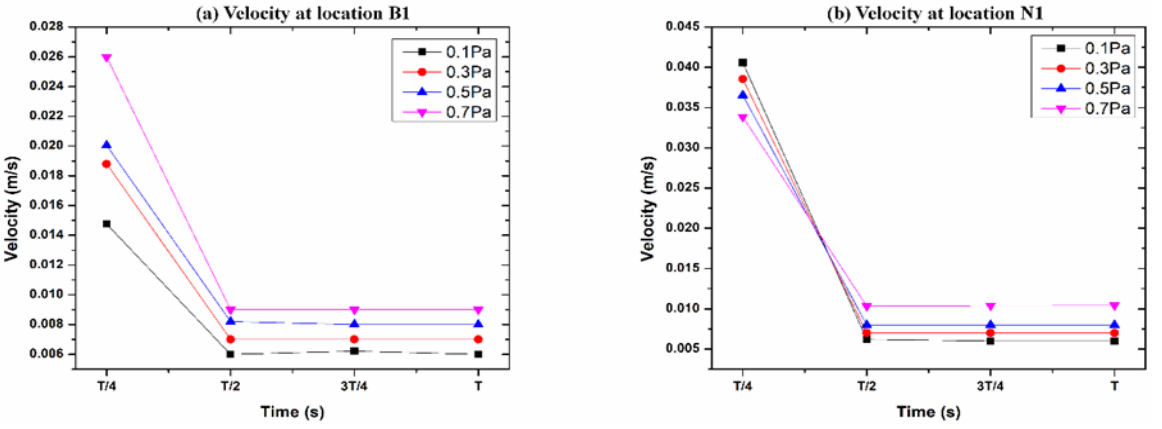

Fig. 8 (a) Velocity at the location B1 of bolus center; (b) Velocity at N1 at bolus neck center.

Table 2. The results of pressure magnitude at the bolus and neck for the input pressure of 0.7 Pa and 0.1 Pa.

Time	Location (bolus)	pressure magnitude (Pa) for input pressure of 0.7 Pa	Location (Neck)	Pressure magnitude (Pa) for input pressure of 0.1 Pa
T/4 s	B1	1.28	N1	-1.03
T/2 s	B2	0.931	N2	-1.145
3T/4 s	B3	0.622	N3	-1.327
T s	B4	0.34	N4	-1.512

3.3 Velocity at the center of urine bolus and bolus neck

Analysis of peristalsis-induced transport in the ureter has shown that when the contraction starts, there is a large backward flow to the kidney at the entrance of the ureter. The velocity was plotted at an inlet pressure of 0.1 Pa, 0.3 Pa, 0.5 Pa, and 0.7 Pa for the time steps, T/4, T/2, 3T/4, and T at the bolus and neck center, where B1, B2, B3, and B4 are bolus center locations. Similarly, N1, N2, N3, and N4 are bolus neck centers as shown in Fig. 3.

During the peristalsis wave propagation at time T/4 s, the maximum magnitude of velocity travels from UPJ to the contraction region near the symmetry line. It is observed that the maximum velocity of 0.0406 m/s at N1 and B1 and the minimum velocity of 0.0148 m/s for the input of 0.1 Pa are recorded as shown in Figs. 8(a & b). At Bolus neck (N1) due to the contraction of the wall by the peristalsis wave maximum

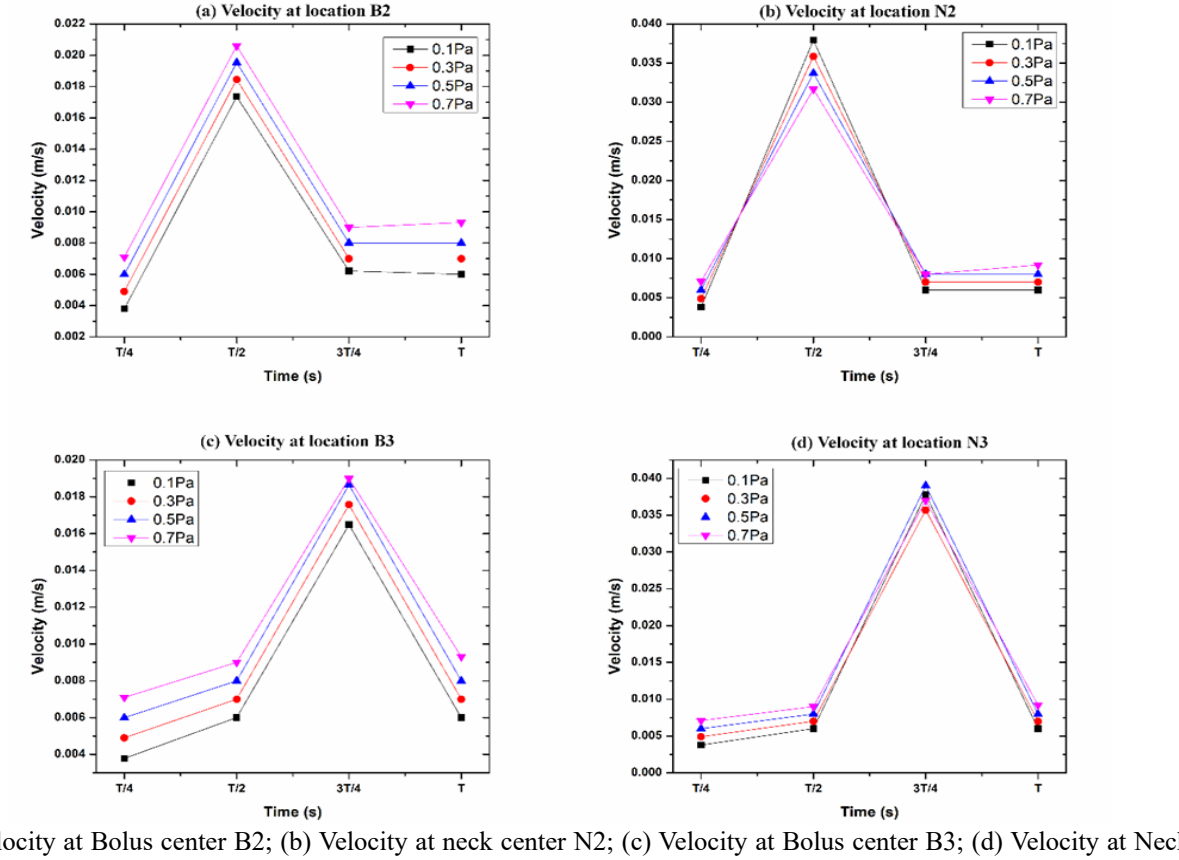

Fig. 9 (a) Velocity at Bolus center B2; (b) Velocity at neck center N2; (c) Velocity at Bolus center B3; (d) Velocity at Neck center N3.

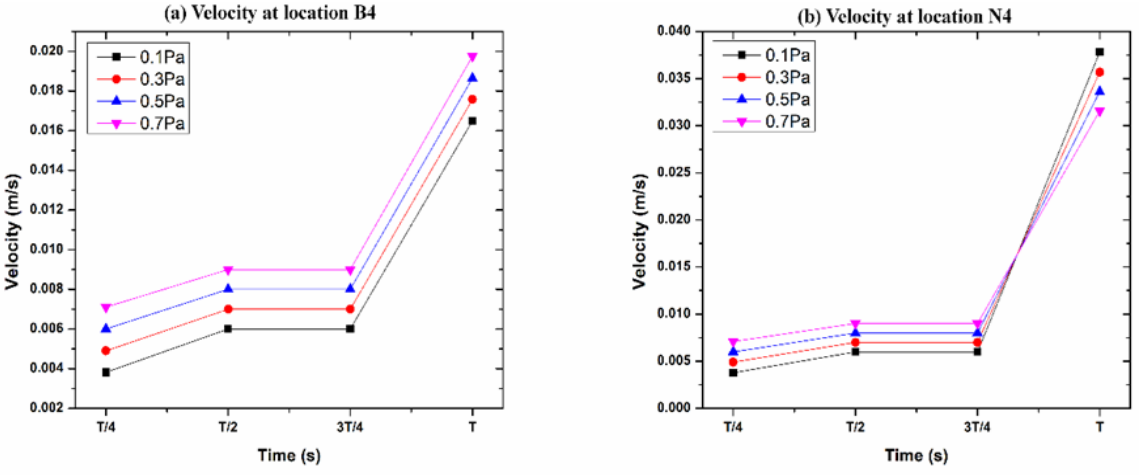

Fig. 10 (a) Velocity at location B4 of bolus center; (b) Velocity at N4 at bolus neck center.

velocity is recorded downstream of the flow (Fig. 8(b)).

As the peristalsis wave is at the middle of the ureter which is at location B2 and N2 at time T/2 s. A maximum velocity of 0.038 m/s and a minimum of 0.017 m/s are recorded at the N2 and B2, respectively, for the inlet pressure of 0.1 Pa as shown in Figs. 9(a & b). Similarly, at locations, B3 and N3 same magnitude of B2 and N3 is observed as shown in Figs. 9(c & d). The condition of ureter contraction with a low-velocity magnitude does not have an evident effect on the urine velocity magnitude. Therefore, in these cases, the peristaltic mechanism does not have a noticeable effect on the ureteral outlet flow. Bahman *et al.*[34] report the contraction wave with a higher velocity has a noticeable effect on the outlet flow.

At the last location of the ureter, for the time T s maximum velocity of 0.038 m/s and a minimum of 0.017 m/s is found at the N4 and B4 respectively. This maximum velocity is observed due to the outlet boundary condition and contraction of the ureter wall. Figs. 10(a & b) show the velocity at location B4 of the bolus center and N4 at the bolus neck center.

Table 3. The results of velocity magnitude at the bolus and neck for the input pressure of 0.7 Pa and 0.1 Pa.

Time	Location (bolus)	Velocity magnitude (Pa) for input pressure of 0.7 Pa	Location (Neck)	Velocity magnitude (Pa) for input pressure of 0.1 Pa
T/4 s	B1	0.026	N1	0.042
T/2 s	B2	0.020	N2	0.038
3T/4 s	B3	0.019	N3	0.038
T s	B4	0.019	N4	0.038

Table 3 shows the results of velocity magnitude at the bolus and neck for the input pressure of 0.7 Pa and 0.1 Pa, respectively. With the initiation of wave motion inside the ureter the maximum velocity is observed at T/4 s. The magnitude tends to decrease as the wave propagates in the ureter along with its length. It is observed that there is a velocity decrease of 26% and 9% in the bolus and neck region, respectively. This velocity decrease is observed during the flow time T/4 s to T s. This study clearly shows that peristaltic motion does not affect the magnitude of the velocity associated with urine bolus, however, it creates sufficient pressure difference to facilitate the motion of bolus in the wave packet form.

4. Conclusion

The current study clearly showed that there is reflux of urine that takes place at the inlet of the ureter due to contraction in an area created by peristalsis wave motion. However as in the current study, it is considered for single wave motion, further multiple wave motions could be considered for the same to know the effect of multiple number wave motion on the reflux of urine. The length of the ureter was considered 275 mm throughout the study. But as per the reported literature, an adult man's ureter length varied from 150 mm to 290 mm. So, for a better understanding, multiple models with changes in the ureter lengths could be used to know the effect of the ureter length on the reflux phenomenon. In the current study, the ureter was considered elastic. Further, Fluid-structure interaction was performed to know the effect of fluid interaction on the ureter wall. Peristalsis wave motion formed due to urine bolus in the ureter was analyzed for single wave motion. The peristalsis mechanism on the ureteral wall was evaluated at different time intervals. The results showed that maximum pressure generates behind the propagating bolus at the time of T/4 s, and the negative pressure developed downstream of the flow. Different inlet pressures of 0.1 Pa, 0.3 Pa, 0.5 Pa, and 0.7 Pa were considered to analyze the pressure and velocity pattern in the ureter bolus and neck. It was found to be a maximum pressure magnitude of 1.28 Pa for an inlet pressure of 0.7 Pa at the time interval of T/4 s. A minimum pressure of -1.512 Pa was found to be at an inlet pressure of 0.1Pa at the time, T s. The peristaltic motion from T/4 s to T s leads to an increase in the negative pressure of 43% for the lower inlet pressure of 0.1 Pa. This showed that there is a tendency to be reversed during the peristalsis motion. Reverse flow due to negative pressure will develop the urinary tract

infection in the ureter and results in the bacteria and toxins from the ureter into the renal pelvis and kidneys. This may further lead to serious kidney problems over some time. Also, it was observed that the maximum velocity magnitude of 0.0406 m/s at the time T/4 s for the input pressure of 0.1 Pa. The velocity for the other timesteps was constant. The minimum velocity required was 0.0148m/s. The peristaltic motion does not affect the magnitude of the velocity associated with urine bolus however it creates sufficient pressure difference to facilitate the motion of bolus in the wave packet form. Further, prototype models can be used to validate the results in in-vitro conditions. This helps clinicians to understand the bouls movement in the ureter.

Acknowledgments
The authors thank the Department of Aeronautical and Automobile Engineering, Manipal Institute of Technology, Manipal Academy of Higher Education (MAHE), Manipal for providing the high computational facility to carry out this research.

Conflict of interest
The authors declare no conflict of interest.

Supporting information
Not applicable.

Abbreviations
FSI - Fluid-structure interaction
FEM - Finite element method
UPJ - Ureteropelvic junction
UVJ - Ureterovesical junction
u_f - Velocity vector
p - Pressure
ρ - Density
μ - Fluid dynamic viscosity
k - Wave number
ω - Frequency.

References
[1] F. Kiil, Urinary flow and ureteral peristalsis. Urodynamics. Berlin, *Heidelberg: Springer Berlin Heidelberg*, 1973, 57-70, doi: 10.1007/978-3-642-65640-8_10.
[2] H. M. Rasouly, W. Lu, Lower urinary tract development and disease, *Wiley Interdisciplinary Reviews: Systems Biology and Medicine*, 2013, **5**, 307-342, doi: 10.1002/wsbm.1212.
[3] A. Kondo, The Contraction of The Ureter I. Observations in Normal Human and Dog Ureters, *Nagoya Journal Medical Science,* 1970, **32**, 387-394.
[4] B. Vahidi, N. Fatouraee, A numerical simulation of peristaltic motion in the ureter using fluid structure interactions, *29th Annual International Conference of the IEEE Engineering in Medicine and Biology Society*, 2007, 1168-1171, doi: 10.1109/IEMBS.2007.4352504.
[5] D. R. Hickling, T.-T. Sun, X.-R. Wu, Anatomy and physiology of the urinary tract: relation to host defense and microbial infection, *Microbiology Spectrum*, 2015, **3**, 1-25, doi: 10.1128/microbiolspec.uti-0016-2012.
[6] Kill, *Irish Journal of Medical Science*, 1958, **33**, 64-64, doi: 10.1007/BF02951244.
[7] D. J. Griffiths, Flow of urine through the ureter: a collapsible, muscular tube undergoing peristalsis, *Journal of Biomechanical Engineering*, 1989, **111**, 206-211, doi: 10.1115/1.3168367.
[8] A. C. Kinn, Progress in urodynamic research on the upper urinary tract: implications for practical urology, *Urological Research*, 1996, **24**, 1-7, doi: 10.1007/BF00296725.
[9] L.G. Keni, S. Kalburgi, M. Zuber, Z. Hammed, M. S. S. Tamagawa, S. Shenoy, Finite Element Analysis of Urinary Bladder Wall Thickness at Different Pressure Condition, *Journal of Mechanics in Medicine and Biology*, 2019, **19**, 1950029, doi: 10.1142/S0219519419500295.
[10] J. C. Burns, T. Parkes, Peristaltic motion, *Journal of Fluid Mechanics*, 1967, **29**, 731-743, doi: 10.1017/S0022112067001156.
[11] C. H. Li, Peristaltic transport in circular cylindrical tubes, *Journal of Biomechanics*, 1970, **3**, 513-523, doi: 10.1016/0021-9290(70)90060-6.
[12] T.-F. Zien, S. Ostrach, A long wave approximation to peristaltic motion, *Journal of Biomechanics*, 1970, **3**, 63-75, doi: 10.1016/0021-9290(70)90051-5.
[13] E. Bruijnes, The Ureteral Pressure Profile, *Urologia Internationalis*, 1978, **33**, 381-392, doi: 10.1159/000280227.
[14] A. Shafik, Ureteric Profilometry: A study of the ureteric pressure profile in the normal and pathologic ureter, *Scandinavian Journal of Urology and Nephrology*, 1998, **32**, 14-19, doi: 10.1080/003655998750014620.
[15] B. Vahidi, N. Fatouraee, Mathematical modeling of the ureteral peristaltic flow with fluid structure interaction, *Journal of Biomechanics*, 2007, **40**, doi: 10.1016/S0021-9290(07)70219-1
[16] L. Knudsen, H. Gregersen, B. Eika, J. Frøkiær, Elastic wall properties and collagen content in the ureter: an experimental study in pigs, *Neurourology and Urodynamics*, 1994, **13**, 597-606, doi: 10.1002/nau.1930130515.
[17] D. P. Sokolis, Multiaxial mechanical behaviour of the passive ureteral wall: experimental study and mathematical characterisation, *Computer Methods in Biomechanics and Biomedical Engineering*, 2012, **15**, 1145-1156, doi: 10.1080/10255842.2011.581237.
[18] G. Hosseini, J. J. R. Williams, E. J. Avital, A. Munjiza, X. Dong, J. S. A. Green, *Simulation of the upper urinary system, Critical Reviews in Biomedical Engineering*, 2013, **41**, 259-268, doi: 10.1615/critrevbiomedeng.2013009704.
[19] Z. Najafi, P. Gautam, B. F. Schwartz, A. J. Chandy, A. M. Mahajan, Three-dimensional numerical simulations of peristaltic contractions in obstructed ureter flows, *Journal of Biomechanical Engineering*, 2016, **138**, 101002, doi: 10.1115/1.4034307.
[20] A. Rassoli, M. Shafigh, A. Seddighi, A. Seddighi, H. Daneshparvar, N. Fatouraee, Biaxial mechanical properties of human ureter under tension, *Urology Journal*, 2014, **11**, 1678-

1686.
[21] A. Takaddus, P. Gautham, A. Chandy, Numerical simulations of peristalsis in unobstructed human ureter, *ASME International Mechanical Engineering Congress abd Exposition (IMECE)*, 2016, 1-8, doi: 10.1115/IMECE2016-65999.
[22] B. Vahidi, N. Fatouraee, A. Imanparast, A. N. Moghadam, A mathematical simulation of the ureter: effects of the model parameters on ureteral pressure/flow relations, *Journal of Biomechanical Engineering*, 2011, **133**, 1, doi: 10.1115/1.4003316.
[23] Z. Najafi, B. F. Schwartz, A. J. Chandy, A. M. Mahajan, A two-dimensional numerical study of peristaltic contractions in obstructed ureter flows, *Computer Methods in Biomechanics and Biomedical Engineering*, 2018, **21**, 22-32, doi: 10.1080/10255842.2017.1415333.
[24] K. N. Chethan, M. Zuber, S. N. Bhat, S. B. Shenoy, Comparative study of femur bone having different boundary conditions and bone structure using finite element method, *The Open Biomedical Engineering Journal*, 2018, **12**, 115-134, doi: 10.2174/1874120701812010115.
[25] K. N. Chethan, M. Zuber, S. N. Bhat, S. B. Shenoy, Optimized trapezoidal-shaped hip implant for total hip arthroplasty using finite element analysis, *Cogent Engineering*, 2020, **7**, 1719575, doi: 10.1080/23311916.2020.1719575.
[26] Chetha K N, G. Ogulcan, S. Bhat N, M. Zuber, S. Shenoy B, Wear estimation of trapezoidal and circular shaped hip implants along with varying taper trunnion radiuses using finite element method, *Computer Methods and Programs in Biomedicine*, 2020, **196**, 105597, doi: 10.1016/j.cmpb.2020.105597.
[27] S. Mihçin, S. Ciklacandir, Towards integration of the finite element modeling technique into biomedical engineering education, *Biomedical Engineering: Applications, Basis and Communications*, 2022, **34**, doi: 10.4015/S101623722150054X
[28] A. B. S. Car, S. Mihcin, Vehicle internal design improvement guidelines by using the computational pregnant occupant model 'Expecting', *International Journal of Human Factors Modelling and Simulation*, 2010, **1**, 380, doi: 10.1504/ijhfms.2010.040272
[29] A. Eram, M. Zuber, L. G. Keni, S. Kalburgi, R. Naik, S. Bhandary, S. Amin, I. A. Badruddin, Finite element analysis of immature teeth filled with MTA, Biodentine and Bioaggregate, *Computer Methods and Programs in Biomedicine*, 2020, **190**, 105356, doi: 10.1016/j.cmpb.2020.105356.
[30] K. N. Chethan, S. N. Bhat, M. Zuber, S. B. Shenoy, Finite Element Analysis of Different Hip Implant Designs along with Femur under Static Loading Conditions, *Journal of Biomedical Physics and Engineering*, 2019, **9**, 507-516. doi: 10.31661/jbpe.v0i0.1210
[31] T. S. Kohler, M. Yadven, A. Manvar, N. Liu, M. Monga, The length of the male urethra, *International Brazilian Journal of Urology*, 2008, **34**, 451-456, doi: 10.1590/s1677-55382008000400007.
[32] L. G. Keni, M. J. Hayoz, S. M. A. Khader, P. Hegde, K. Prakashini, M. Tamagawa, B. Satish Shenoy, B. M. Z. Hameed, M. Zuber, Computational flow analysis of a single peristaltic wave propagation in the ureter, *Computer Methods and Programs in Biomedicine*, 2021, **210**, 106378, doi: 10.1016/j.cmpb.2021.106378.
[33] B. Vahidi, N. Fatouraee, A biomechanical simulation of ureteral flow during peristalsis using intraluminal morphometric data, *Journal of Theoretical Biology*, 2012, **298**, 42-50, doi: 10.1016/j.jtbi.2011.12.019.
[34] B. Vahidi, N. Fatouraee, A. Imanparast, A. N. Moghadam, A mathematical simulation of the ureter: effects of the model parameters on ureteral pressure/flow relations, *Journal of Biomechanical Engineering*, 2011, **133**, 031004, doi: 10.1115/1.4003316.
[35] N. P. Khabazi, K. Sadeghy, Peristaltic transport of solid particles suspended in a viscoplastic fluid: a numerical study, *Journal of Non-Newtonian Fluid Mechanics*, 2016, **236**, 1-17, doi: 10.1016/j.jnnfm.2016.08.001.
[36] A. A. Bykova, S. A. Regirer, Mathematical models in urinary system mechanics (review), *Fluid Dynamics*, 2005, **40**, 1-19, doi: 10.1007/s10697-005-0039-y.
[37] S. V. Patankar, Numerical Heat Transfer and Fluid Flow, *CRC Press*, 2018, doi: 10.1201/9781482234213.
[38] J. N. J. Lozano, Peristaltic flow with application to ureteral biomechanics, *University of Notre Dame, Indiana*, USA, 2009, 195.
[39] S. L. Weinberg, Ureteral function. I. Simultaneous monitoring of ureteral peristalsis, *Investigative Urology*, 1974, **12**, 103-107.
[40] P. S. Lykoudis, 16 - The Ureter as a Peristaltic Pump, *Urodynamics*, 1971, 199-215, doi: 10.1016/B978-0-12-121250-6.50023-X.
[41] M. S. Najar, C. L. Saldanha, K. A. Banday, Approach to urinary tract infections, *Indian Journal of Nephrology*, 2009, **19**, 129, doi: 10.4103/0971-4065.59333.
[42] A. L. Flores-Mireles, J. N. Walker, M. Caparon, S. J. Hultgren, Urinary tract infections: epidemiology, mechanisms of infection and treatment options, *Nature Reviews Microbiology*, 2015, **13**, 269-284, doi: 10.1038/nrmicro3432.
[43] G. Hosseini, C. Ji, D. Xu, M. A. Rezaienia, E. Avital, A. Munjiza, J. J. R. Williams, J. S. A. Green, A computational model of ureteral peristalsis and an investigation into ureteral reflux, *Biomedical Engineering Letters*, 2018, **8**, 117-125, doi: 10.1007/s13534-017-0053-0.

Author Information

Mr. Laxmikant G K *received Mechanical Engineering from Visweswariah Technological University, Karnataka. He completed his Masters's Degree in Computer-Aided Mechanical Design and Analysis from Manipal Institute of Technology Manipal. Pursuing his Ph.D. on ureter flow dynamics from Manipal Academy of Higher Education. His areas of interest are Fluid-Structure Interaction, Computational Bio-fluid Mechanics, Computational fluid*

dynamics, Structural Analysis, and Machine Design. Currently, he is working as Assistant Professor-Senior Grade at the Department of Aeronautical and Automobile Engineering.

***Dr. Satish Shenoy B** working as a Professor in the Department of Aeronautical and Automobile Engineering, Manipal Institute of Technology, Manipal Academy of Higher Education, Manipal, Karnataka, INDIA. He holds B. E. (Mechanical Engineering), M. Tech (Manufacturing Engineering & Technology), and Ph.D. (Tribology) degrees. He has more than twenty of teaching and research experience. His area of interest includes Biomechanics of the hip joint, Finite element analysis of biomedical implants, Composite materials, Manufacturing of medical implants, Computational fluid dynamics.*

***Dr. Padmaraj Hegde** is one of the popular doctors in the Department of Urology at Kasturba Hospital, Manipal. He has completed his M.B.B.S, M.S. (Gen Surgery), and MCh (Urology) from the prestigious Kasturba Medical College, Manipal under Manipal Academy of Higher Education. He obtained a Fellow of the Royal College of Surgeons, Glasgow University, and Fellow of the International Medical Sciences Academy. Dr. Hegde is associated with the Department of Urology, KMC Manipal for the last 21 years and has vast experience in treating patients with urological conditions. He has a keen interest in Andrology, Stone disease, Endourology, and Male Infertility. Presently he is the Professor of Urology and Heading Unit at Kasturba medical college Hospital, Manipal.*

***Dr. Prakashini K** graduated in Medicine from Manipal Academy of Higher Education, Manipal. She completed her M.D in Radiodiagnosis from the same institute. Dr. Prakashini is presently working as a Professor and Head in the Department of Radio-Diagnosis and Imaging, Kasturba Hospital, Manipal University. Her core expertise is in the domain of Advanced Ultrasound Imaging, Cardiovascular Imagining. She has several publications in the area of Cardiovascular and Abdominal Imaging.*

***Dr. Mohammad Zuber** graduated in Mechanical Engineering from Visweswariah Technological University, Karnataka. He completed his Masters's Degree in Thermal Engineering system Technology. Completed his Ph.D. on biofluid dynamics from Universiti Sains Malaysia. His areas of interest are Fluid-Structure Interaction, Computational Bio-fluid Mechanics, CFD, Aerodynamics, and Biomimetics. He has worked as Post Doc Fellow at Universiti Sains Malaysia, Malaysia. He has also worked as Senior Lecturer at Dept. of Aerospace Engineering, Universiti Putra Malaysia, from 2014 to 2017. Currently, he is the Assistant Director for Innovation & Incubation at Manipal Institute of Technology, Manipal.*

***Dr. S. M Abdul Khader** obtained Mechanical Engineering from Visweswariah Technological University, Karnataka. He completed his Masters's Degree in Computer-Aided Mechanical Design and Analysis from Manipal Institute of Technology Manipal. Earned his Ph.D. degree in biofluid dynamics from Manipal University. His areas of interest are Fluid-Structure Interaction, Computational Bio-fluid Mechanics, CFD, Structural Analysis, and Machine Design. Currently, he is working as Associate Professor Department of Mechanical and Manufacturing Engineering.*

***Dr. Massaki Tamagawa** obtained a Bachelor of Engineering in Mechanical Engineering from the Faculty of Engineering, Kyoto University, Japan. He completed his Masters's Degree in Mechanical Engineering from the Faculty of Engineering, The University of Tokyo (Institute of Industrial Science), Japan. Earned his Ph.D. degree from the Department of Mechanical Engineering, Faculty of Engineering, Kyoto University, Japan. His areas of interest are Computational Bio-fluid Mechanics and Biomimetics. Currently, he is a professor at the Faculty of Engineering, Kyoto University, Japan.*

***Zeeshan Hameed BM** is a Professor in the Department of Urology, Father Muller Medical College, Mangalore, India. His research interests include studies about urological malignancies, artificial intelligence, and design and product*

development techniques. He has applied for 3 patents at Indian Patent Office. He has published several research publications in international journals of repute and has a keen interest in medical innovations. His areas of expertise include medical devices and innovations, artificial intelligence, and medical web and app development. He has developed a web application for urological stent and symptom tracking by the name "UROSTENTZ".

